Classification of Voronoi and Delone tiles of quasicrystals: II. Circular acceptance window of arbitrary size

2003 J. Phys. A: Math. Gen. 36 1895

(http://iopscience.iop.org/0305-4470/36/7/307)

INSTITUTE OF PHYSICS PUBLISHING JOURNAL OF PHYSICS A: MATHEMATICAL AND GENERAL

J. Phys. A: Math. Gen. **36** (2003) 1895–1912 PII: S0305-4470(03)39943-3

Classification of Voronoi and Delone tiles of quasicrystals: II. Circular acceptance window of arbitrary size

Z Masáková[1], **J Patera**[2] **and J Zich**[3]

[1] Department of Mathematics, Faculty of Nuclear Sciences and Physical Engineering, Czech Technical University, Trojanova 13, 120 00 Praha 2, Czech Republic
[2] Centre de Recherches Mathématiques, Université de Montréal, CP 6128, succursale centre-ville, Montréal, Québec, Canada H3C 3J7
[3] Department of Mathematics, Faculty of Nuclear Sciences and Physical Engineering, Czech Technical University, Trojanova 13, 120 00 Praha 2, Czech Republic

E-mail: masakova@km1.fjfi.cvut.cz, patera@crm.umontreal.ca and zich@kaktus.cz

Received 24 July 2002, in final form 9 December 2002
Published 5 February 2003
Online at stacks.iop.org/JPhysA/36/1895

Abstract

In this paper we describe all the Voronoi and Delone tiles arising in tilings of point sets $\Sigma(\Omega)$ ('quasicrystals') built by the standard projection of the root lattice of type A_4 onto a two-dimensional plane spanned by the roots of the Coxeter group H_2 (dihedral group of order 10). The acceptance window Ω for $\Sigma(\Omega)$ is a disc of any radius $0 < r < \infty$. There are 22 distinct sets VT_j $(j = 1, \ldots, 22)$ of Voronoi tiles and eight sets DT_k $(k = 1, \ldots, 8)$ of Delone tiles, up to a uniform scaling by a factor τ^n where $\tau = \frac{1}{2}(1 + \sqrt{5})$ is the golden ratio and $n \in \mathbb{Z}$.

PACS number: 61.44.Br

1. Introduction

Tessellations, or equivalently tilings, of an Euclidean plane, found as mosaics and other symmetrical decorations, are subject to relatively restrictive rules, in spite of their apparent variety. Indeed if, as is often the case, they should be invariant with respect to an infinite group of plane isometries, there are precisely 17 groups of possible symmetries, discounting tessellations which are extensions of linear tessellations.

During the last three decades new much richer class of tessellations of an Euclidean plane was found, sharing many properties with the classical symmetrical ones: the new tessellations are deterministic, uniformly dense and uniformly discrete, and there are infinitely many of them, all with abundant symmetry properties. Their most distinctive feature is the complete lack of translation symmetry.

This paper is devoted to a specific problem concerning one of the most common families of the aperiodic tessellations, namely to the description of all the distinct tiles which are found in these tessellations. The main contribution of this paper is the discovery that the family containing uncountably many tessellations, admits just 22 sets of tiles, called here VT_m ($m = 1, \ldots, 22$) and eight of their dual sets DT_k ($k = 1, \ldots, 8$). Depending on the specific conditions of a particular case, each set may appear uniformly scaled by an integer power of a constant. In all the tessellations of the family, there are 17 different shapes of tiles in VT sets and four shapes in DT sets, up to a scaling and rotation.

The family of tilings, considered here, arises from a point set $\Sigma(\Omega)$ as its Voronoi and Delone tilings. The point set is the result of a standard projection of a slice of the root lattice of A_4 type onto a two-dimensional subspace oriented in such a way that the irrationality $\tau = \frac{1}{2}(1+\sqrt{5})$ appears in the coordinates of the projected lattice points. The slice of the root lattice is fixed by the choice of Ω. Details of the construction of Σ have been described many times, most recently in [1].

The present paper and the subsequent one [2] are the first applications of the method, developed in [1], respectively to tilings of quasicrystals with circular and decagonal acceptance window of any size. Since the quasicrystal models considered here have the scaling symmetry with the self-similarity factor τ, the problem of this paper reduces to the description of tiles in quasicrystals whose acceptance window is a disc of radius within the range $(\tau^{-1}, 1]$. Notation and most of the conventions used here coincide with those of [1]. For further questions concerning the method, literature and some motivation, we refer the reader to [1]. Our aim in writing this paper was to make it self-contained for understanding the results. However, for following up the procedure to arrive at these results, one needs to consult [1].

2. Basic setup for circular window

Through the text we use the following constants and related identities:

$$\tau = \tfrac{1}{2}(1+\sqrt{5}) \qquad \tau' = \tfrac{1}{2}(1-\sqrt{5}) \qquad \tau+\tau' = 1 \qquad \tau\tau' = -1.$$
$$\Delta = \sqrt{(2+\tau)} \qquad \Delta^* = \sqrt{(2+\tau')} \qquad \Delta^2 + (\Delta^*)^2 = 5 \qquad \Delta\Delta^* = \sqrt{5} = \tau - \tau'.$$

There are two two-dimensional real Euclidean spaces involved in the construction of the (cut and project) point sets, whose Voronoi and Delone tiles we want to list. Denote them by V_1 and V_2. They are spanned by the bases $\{\alpha_1, \alpha_2\}$ and $\{\alpha_1^*, \alpha_2^*\}$, respectively, where the bases are specified by their respective Gram matrices:

$$((\alpha_j|\alpha_k)) = \begin{pmatrix} 2 & -\tau \\ -\tau & 2 \end{pmatrix} \qquad ((\alpha_j^*|\alpha_k^*)) = \begin{pmatrix} 2 & -\tau' \\ -\tau' & 2 \end{pmatrix}.$$

Crucial for our construction is the star map between V_1 and V_2. It is defined only for dense subsets $M \subset V_1$ and $M^* \subset V_2$, consisting of points with coordinates of the form $a+\tau b$, where $a, b \in \mathbb{Q}$, relative to our chosen bases, i.e. M (resp. M^*) is the integer span of the root system Δ_2 of the Coxeter group H_2. In this paper we encounter only integers a and b. The star map is given by

$$M \longleftrightarrow M^*: \quad x = (a+\tau b)\alpha_1 + (c+\tau d)\alpha_2 \quad \longleftrightarrow \quad x^* = (a+\tau' b)\alpha_1^* + (c+\tau' d)\alpha_2^*.$$

The point sets $\Sigma(\Omega)$ of interest to us ('quasicrystals') are defined as follows [3]:

$$\Sigma(\Omega) := \{x \in M \mid x^* \in \Omega\}.$$

In this paper Ω is always the disc of radius $0 < r < \infty$ which is centred at the origin. Since the quasicrystals satisfy $\tau\Sigma(\Omega) = \Sigma(\tau'\Omega)$, we can reduce our considerations without loss of generality to the values of radius r within the range $r \in (\tau^{-1}, 1]$.

Table 1. Calculations of Voronoi and Delone tilings for circular acceptance window are divided into three cases. Auxiliary results for the cases are listed.

	Case 1	Case 2	Case 3
Value of r	$\left(\frac{1}{\tau}, \frac{\tau\Delta}{4}\right]$	$\left(\frac{\tau\Delta}{4}, \frac{\tau}{2}\right]$	$\left(\frac{\tau}{2}, 1\right]$
Value of d_1	$\left(\frac{4}{\tau\Delta}, \tau\right]$	$\left(\tau, \frac{2\tau}{\Delta}\right]$	$\left(\frac{2\tau}{\Delta}, \frac{4}{\Delta}\right]$
Value of d_2	$\left(\frac{2}{\tau^2}, \frac{\Delta}{2}\right]$	$\left(\frac{\Delta}{2}, 1\right]$	$\left(1, \frac{2}{\tau}\right]$
Tiles in $\Sigma(I_1)$	$1, \tau, \tau^2$	$1/\tau, 1, \tau$	$1/\tau, 1, \tau$
Tiles in $\Sigma(I_2)$	τ, τ^2, τ^3	τ, τ^2, τ^3	$1, \tau, \tau^2$
R_c for $\Sigma(\Omega_2)$	$\frac{\tau^3}{\Delta}$	$\frac{\tau^3}{\Delta}$	$\frac{\tau^2}{\Delta}$
Value of d	$\frac{8\tau^4}{\Delta}$	$\frac{8\tau^4}{\Delta}$	$\frac{8\tau^3}{\Delta}$
Value of n	5	10	5
$\lvert\mathcal{L}_{2n}(I_1, I_2)\rvert$	43	75	43
$\lvert\widetilde{\mathcal{N}}\rvert = (8n+3)^2$	1849	5625	1849

Let $x \in \Sigma(\Omega)$. Then the Voronoi cell (or domain or tile) $V(x)$ is defined as

$$V(x) := \{y \in V_1 \mid |x - y| \leqslant |y - z| \text{ for all } z \in \Sigma(\Omega)\}.$$

Thus there is precisely one quasicrystal point in the interior of any Voronoi tile and none on its boundary.

In order to apply the general method of [1] to the specific case of quasicrystals with circular acceptance window, we have to make some preliminary considerations. We shall make some comments on the calculations needed and gather the results in table 1. In order to avoid repetitions, we refer the reader for details of the method to section 5 of [1]. According to this method, we first have to compute the sizes of rhombuses, denoted respectively by Ω_1 and Ω_2, which are inscribed and described to the disc Ω. Let Ω_i be the Cartesian product $I_i \times I_i$ of intervals I_i of length d_i, $i = 1, 2$. One can easily verify that

$$d_1 = \frac{r}{\cos\frac{\pi}{5}\sin\frac{\pi}{5}} = \frac{4r}{\Delta} \qquad d_2 = \frac{r}{\cos\frac{\pi}{5}} = \frac{2r}{\tau} \qquad \text{i.e.} \quad d_2 = d_1 \sin\frac{\pi}{5} = d_1\frac{\Delta}{2\tau}. \tag{1}$$

The next problem is to compute the covering radius for $\Sigma(\Omega)$ or to find an upper bound for it. Since $\Sigma(\Omega_2) \subset \Sigma(\Omega)$, the covering radius for $\Sigma(\Omega)$ is smaller than that for $\Sigma(\Omega_2)$, $R_c = L/\Delta$, where L is the largest tile in $\Sigma(I_2)$ and depends on the value of r.

- The method (step 1) requires us to compute the value of d which is the side length of the smallest rhomb oriented along the axes α_1, α_2 that contains a circle of radius $2R_c$. It turns out that $d = 8\tau R_c$.
- In step 2 of the method, the value of the covering radius is used to estimate the longest (measured in the number of tiles) possible section in $\Sigma(I_1)$ which fits into $d/2$. The lengths of the tiles in $\Sigma(I_1)$ depend on the actual value of r. In order to determine the right sequence of the tiles, we use some rules for ordering the tiles in a one-dimensional quasicrystal, e.g., that two shortest tiles are never adjacent, etc. The maximal number of tiles that can fit into the length $d/2$ is denoted by n.
- At step 3 of the method we need to find the set of words $\mathcal{L}_{2n}(I_1, I_2)$ introduced in [1]. For that we use the algorithm presented in [5].

- According to the above and steps 5 and 6 of the method, we can determine all local configurations of points in the skeleton (the quasilattice $\Sigma(\Omega_1)$ with points of the subquasicrystal $\Sigma(\Omega_2)$ marked) within the disc of radius $2R_c$. The set of configurations is denoted by $\widetilde{\mathcal{N}}$ as in [1]. The cardinality of this set can be derived from the number of one-dimensional sections in $\mathcal{L}_k(I_1, I_2)$, which is $4k + 3$, see [5]. We are interested in $k = 2n$, i.e. the number of configurations in the skeleton is $|\widetilde{\mathcal{N}}| = (8n + 3)^2$.

Such calculations lead us to the conclusion that we have to divide the considerations into three cases, according to the values of $r \in (\tau^{-1}, 1]$. For the three cases the tiles in $\Sigma(I_1)$, $\Sigma(I_2)$ and consequently all the studied parameters differ. The summary of the results is found in table 1.

3. Related algorithms

Suppose that we have already computed the set $\widetilde{\mathcal{N}}$ of local configurations of the size of the ball with radius $2R_c$ from the skeleton.

Recall that the configurations in $\widetilde{\mathcal{N}}$ contain points $\circ$ from the dense quasi-lattice $\Sigma(\Omega_1)$ and points $\bullet$ belonging also to the sparse quasi-lattice $\Sigma(\Omega_2)$. Every such skeleton configuration determines a set $\mathcal{N}$ of configurations, or the Voronoi tiles, according to steps 7–10 of the method. The points $\circ$ are chosen in every possible way to form a configuration. The configuration then determines a Voronoi tile of the central point. However, not all points of the configuration may actually shape the tile. Therefore, the idle points are finally omitted.

If the number of non-decorated points $\circ$ is k, then the number of configurations to consider is 2^k, although at the end the number of Voronoi tiles in $\mathcal{N}$ is much lower. Practically, it turns out that k may vary up to more than 30, so that it is impossible to enumerate all the 2^k possibilities, since the computation time would exceed months or years. We have, therefore, developed a faster technique: an algorithm based on tree processing. It is illustrated in figure 1.

The idea of the algorithm is to construct $\mathcal{N}$ and simultaneously Voronoi polygons by a recursive procedure, in which we avoid considering two different configurations which shape the same Voronoi tile. The different Voronoi polygons are then saved in a binary tree structure to get the fastest possible comparison.

Suppose that a configuration from $\widetilde{\mathcal{N}}$ is given. Denote the dense points $\circ$ by $1, \ldots, k$. The arguments of recursive procedure are the following—a Voronoi polygon V, a dense point $l \in \{1, \ldots, k\}$ and a flag F. If the flag F is set, then the procedure adds the point l to the neighbours of V. If l does not influence the shape of V, the procedure stops. Otherwise it adds this new polygon $\tilde{V}$ to the output list of polygons. At the end it calls itself recursively twice with the parameters $(\tilde{V}, l + 1, F = \text{set})$ and $(\tilde{V}, l + 1, F = \text{unset})$.

The algorithm requires comparison of constructed Voronoi polygons. We used a simple binary tree, with an order of Voronoi polygons defined as the lexicographic ordering of integer coordinates of the neighbours determining the Voronoi polygon, considered clockwise. This was possible since the neighbours belong to the set $(\mathbb{Z} + \mathbb{Z}\tau)\alpha_1 + (\mathbb{Z} + \mathbb{Z}\tau)\alpha_2$.

Steps 11–13 of the method allow us to choose among the Voronoi tiles in $\mathcal{N}$ those that appear in the Voronoi tiling for the quasicrystal with given acceptance window. First we need to check whether the star image of the configuration fits into the acceptance window, i.e. if $q_1, \ldots, q_m$ are the neighbours of the tile V, we check whether the set

$$\Omega|_V = \left(\bigcap_{j=1}^{m} (\Omega - q_j^\star) \right) \cap \Omega \tag{2}$$

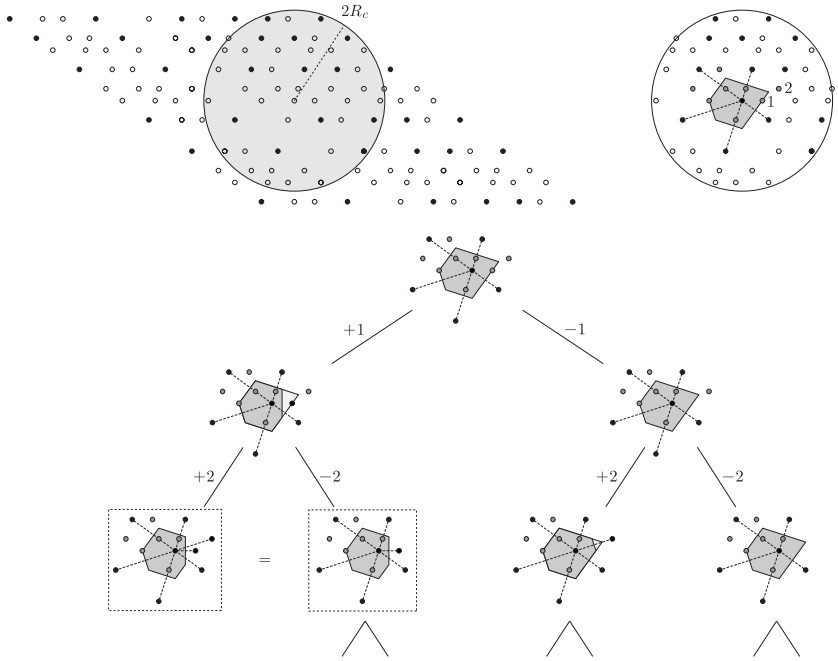

Figure 1. Example of a construction of all Voronoi polygons from one configuration from $\widetilde{\mathcal{N}}$.

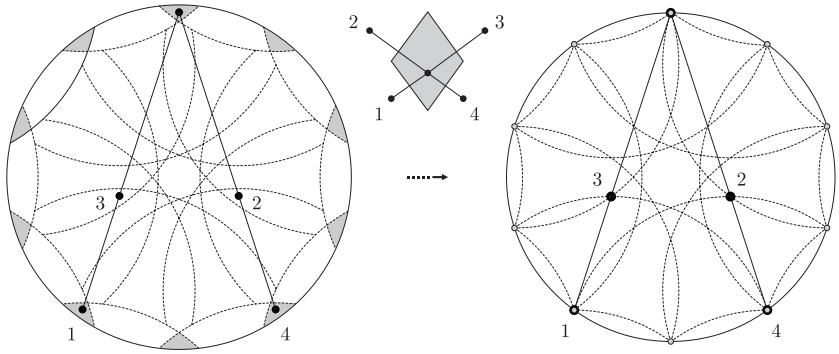

Figure 2. An example of the singular disc acceptance window (on the right) which originates from the non-singular window (on the left) by reducing the radius of the window. Note that the regions of division are slightly deformed while grey parts degenerate to the points. In this singularity the Voronoi tile drawn above disappears because its configuration does not fit into the window.

is empty or not. If $\Omega\,|_V = \emptyset$, then the Voronoi polygon V does not appear in the tiling. We thus have to be able to decide whether an intersection of a finite number of discs with the same radius is empty or not. For two methods of implementation of this problem see [5].

4. Singular cases

So far, the radius of the acceptance disc was fixed within $[\tau^{-1}, 1)$. Suppose now that we want to consider all radii within the finite range. It turns out that the range $[\tau^{-1}, 1)$ gets subdivided into 11 subintervals and that within each subinterval the sets VT and DT do not change. Then we speak of generic or non-singular tiling sets VT and DT. The boundary points of the

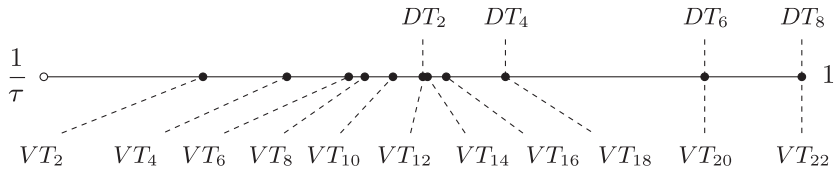

Figure 3. The range $(1/\tau, 1]$ of the radius of the circular acceptance window r divided by singular cases. The figure is drawn in proper scale. Between two Voronoi/Delone singular cases the set of Voronoi/Delone tiles in the tiling does not change.

Table 2. Cases of quasicrystals with circular acceptance windows according to the sets of Voronoi and Delone tiles. There are 22 classes of quasicrystals VT_m, $m = 1, \ldots, 22$, which have different Voronoi tiles. In the second column there are a number of Voronoi shapes in the Voronoi tiling. Even cases are singular and they are represented by quasicrystals with a specific size of window, which is denoted in the middle column. On the other hand, there are only four classes of quasicrystals DT_m, $m = 1, \ldots, 4$, with circular acceptance window, which have different Delone tiles. In the fourth column there are a number of Delone shapes.

VT_1	11			
VT_2	10	$\sqrt{(17-9\tau)/5} \doteq 0.698\,239\,80$		
VT_3	12			
VT_4	11	$(13-3\tau)/11 \doteq 0.740\,536\,18$		
VT_5	12			
VT_6	11	$\sqrt{4-\tau}/2 \doteq 0.771\,680\,96$	5	DT_1
VT_7	13			
VT_8	10	$\sqrt{33-11\tau}/5 \doteq 0.779\,785\,26$		
VT_9	13			
VT_{10}	12	$(4-\tau)/3 \doteq 0.793\,988\,67$		
VT_{11}	13			
VT_{12}	13	$\tau/2 \doteq 0.809\,016\,99$	6	DT_2
VT_{13}	15			
VT_{14}	13	$\sqrt{(13-6\tau)/5} \doteq 0.811\,393\,38$		
VT_{15}	13		6	DT_3
VT_{16}	10	$\sqrt{12-7\tau} \doteq 0.820\,830\,12$		
VT_{17}	10			
VT_{18}	6	$\tau/\Delta \doteq 0.850\,650\,81$	4	DT_4
VT_{19}	7		6	DT_5
VT_{20}	7	$\sqrt{\tau+2}/2 \doteq 0.951\,056\,52$	6	DT_6
VT_{21}	8		7	DT_7
VT_{22}	5	1	5	DT_8

subintervals are the singular values of the radius of the disc, when the sets VT and possibly also DT change. We speak then of singular tiling sets and correspondingly singular tiling of the quasicrystal. Note that there are fewer singular sets DT than singular sets of VT (see figure 3).

Now we will explain how to detect the singular cases of quasicrystals with circular acceptance window. The radius of the acceptance window of the singular quasicrystal has the property that every quasicrystal with larger radius has a different list of Voronoi/Delone tiles than every quasicrystal with arbitrarily smaller radius. Here we explain how the singular cases can be determined from the division of acceptance windows to regions corresponding to different Voronoi tiles.

Suppose we have a circular acceptance window Ω with the radius $r > 0$. For a better illustration see figure 2. Recall that the acceptance window is divided into regions corresponding to different Voronoi tiles, $\Phi(V)$,

$$\Phi(V) = \Omega|_V \setminus \bigcup\{\Omega|_{\tilde{V}} \text{ where } |\tilde{V}| \leqslant |V|\} \tag{3}$$

where sets $\Omega|_V$ are given by formula (2) as intersections of a few shifted discs with the radius r. The centres of these discs are images of neighbours of a given Voronoi tile V, when we suppose that the central point of the Voronoi tile is shifted to the origin. It follows that if the radius r is increased or decreased, the centres of the disc do not move; only the size of the discs around them changes. Thus a singular case occurs if and only if boundaries of two or more discs have exactly one point in common. When a list of Voronoi tiles for the radius r is compiled, it is easy to compute singular cases close to r. For that one can process all pairs and consequently all triplets of discs from which the division is composed and compute for which radius their boundaries intersect at one point. The intersections for singular cases are marked in figures 4–8.

The singularities are illustrated in figure 2. There are two ways to regard the problem. Assume that the Voronoi tile V is given by neighbours $q_1, \ldots, q_m$. Decreasing the radius of the acceptance window may cause such a configuration to no longer fit into the disc. Singular is that value of the radius for which the configuration lies on the boundaries of the disc, as in figure 2. It means that for radii $>r$ the Voronoi tile appears, while for radii $<r$ it does not.

The second way to see a singularity is to observe what happens when we increase the radius of the acceptance window: assume that a Voronoi tile V is given by neighbours $q_1, \ldots, q_m$. When we increase the radius of the disc, it may happen that some new points fit into the acceptance window that influence the shape of the Voronoi tile. Every configuration $q_1, \ldots, q_m$ occurs with these additional points and therefore the tile V does not appear in the tiling for larger radius.

From this it is obvious what role is played by the boundary of the acceptance window. Clearly, the important fact is whether Ω is open or not. It may happen that a tile with zero density appears in the tiling corresponding to the singular value r of the radius. Since the intersection of the disc boundary with the $\mathbb{Z}[\tau]$-lattice M is always finite or empty [4], tiles with zero density appear finitely many times in the tiling. Note also that the position of the acceptance window influences whether the intersection of the boundary with M is empty or not.

Using the calculations of intersections of circles as described above we have discovered that there are 11 singular and 11 non-singular cases according to the Voronoi tiling. The precise values of the corresponding radii are summarized in table 2. Note that there are singular cases which are relatively far and on the other hand some of them are really very close (e.g., VT_{12} and VT_{14}). Simultaneously non-singular case VT_{13} between these two closest singular cases contains the largest number of Voronoi tiles. For these interesting properties a part of its Voronoi and Delone tiling is drawn in figure 9.

The singular cases for Delone tiles were computed analogously. We have to draw the division of the acceptance window according to the different fans of Delone tiles meeting in one central point. More detailed instructions can be found in [1, 5]. The division of the acceptance window according to a fan of Delone tiles is a subdivision of the division according to different Voronoi tiles. Usually, one Delone tile may be present in several fans corresponding to different regions. Therefore, the problem of determining the values of radii for which some Delone tiles appear/disappear in the Delone tiling was slightly more complicated than that for Voronoi tiling. The method was however the same. It turns out that singularities for

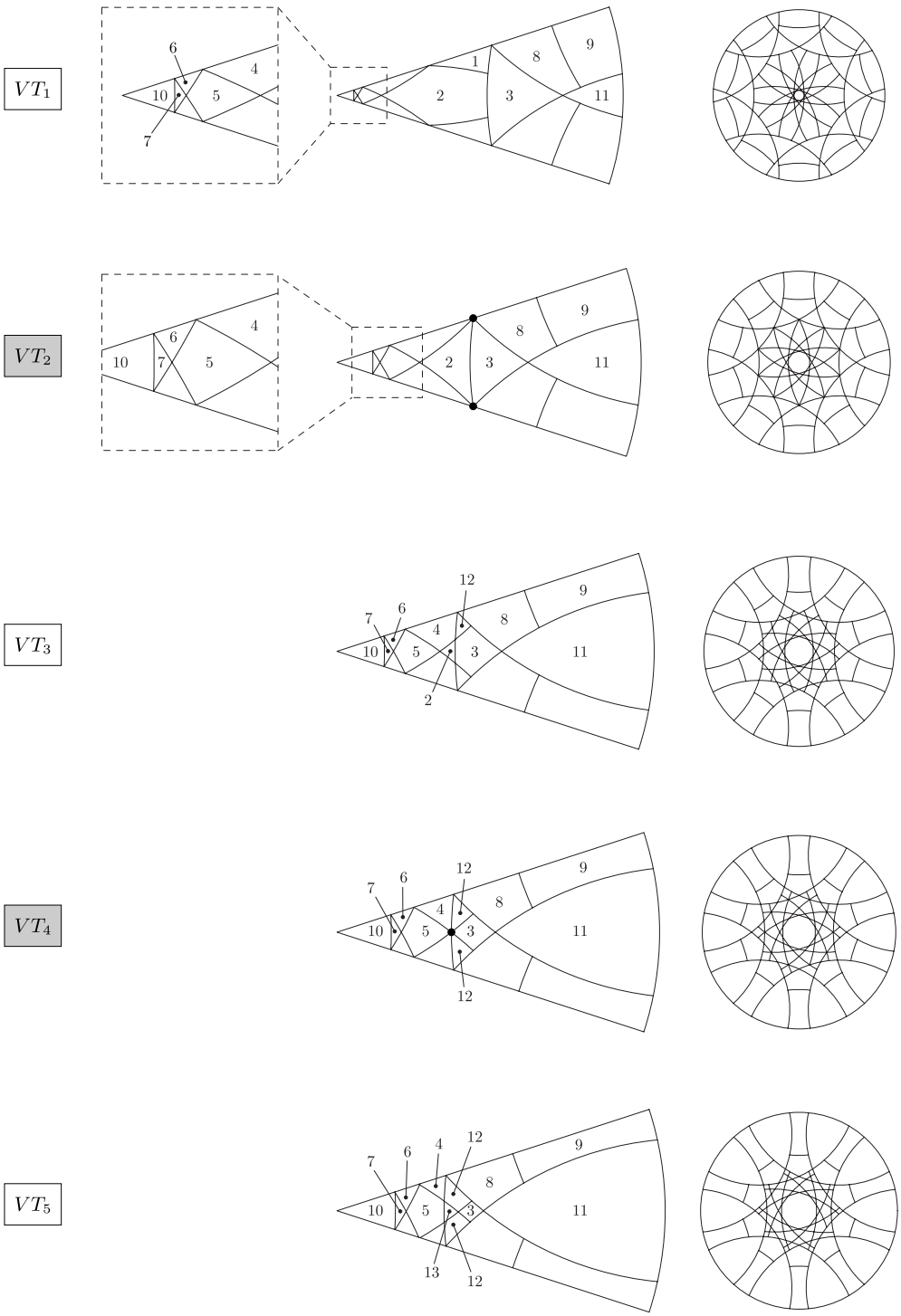

Figure 4. Division of circular acceptance windows (cases VT_1–VT_5). Each region in the acceptance window corresponds to a different Voronoi tile. The numbers which denote these regions are numbers of Voronoi tiles from figure 12.

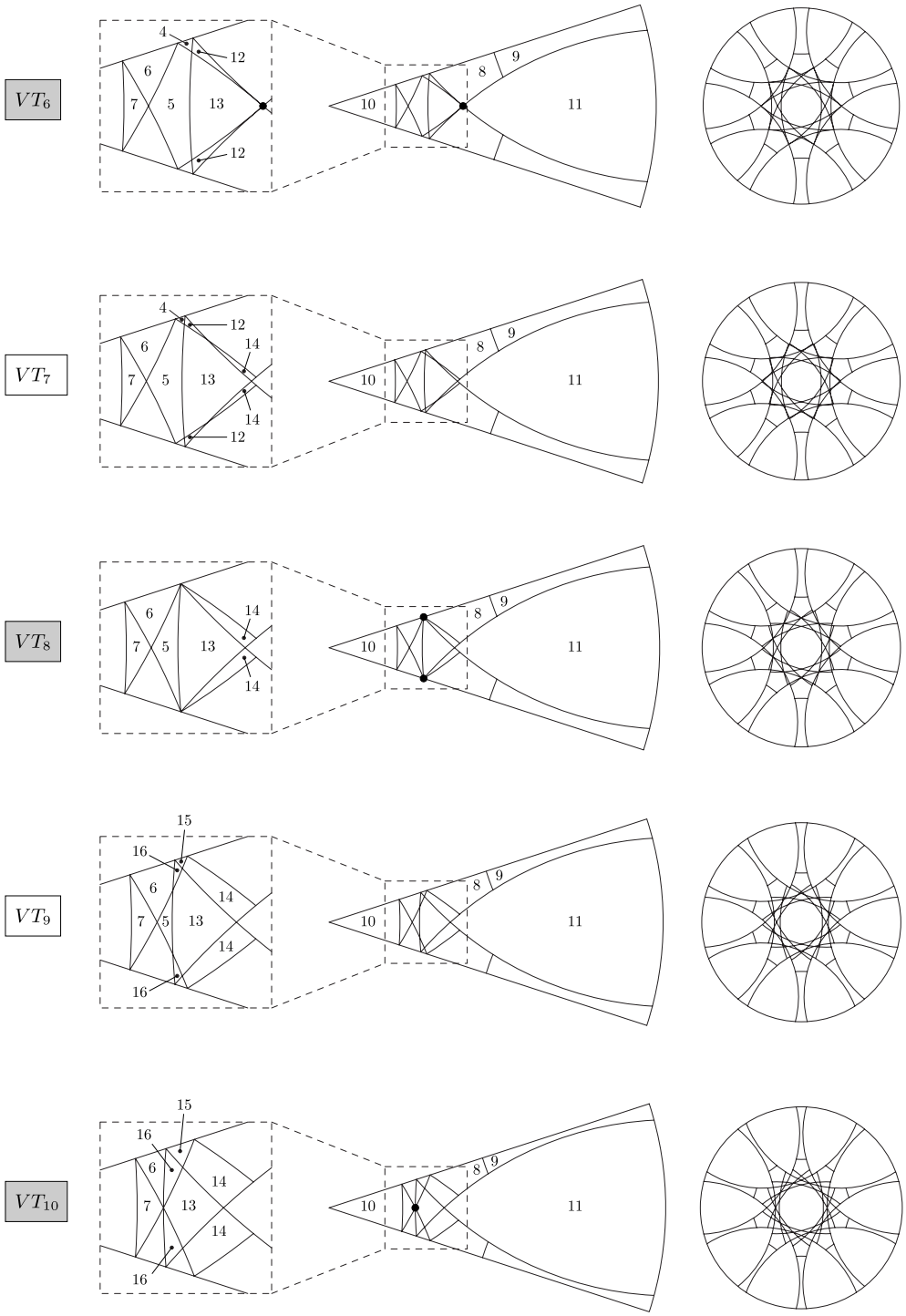

Figure 5. Division of circular acceptance windows (cases VT_6–VT_{10}). Each region in the acceptance window corresponds to a different Voronoi tile. The numbers which denote these regions are the numbers of Voronoi tiles from figure 12.

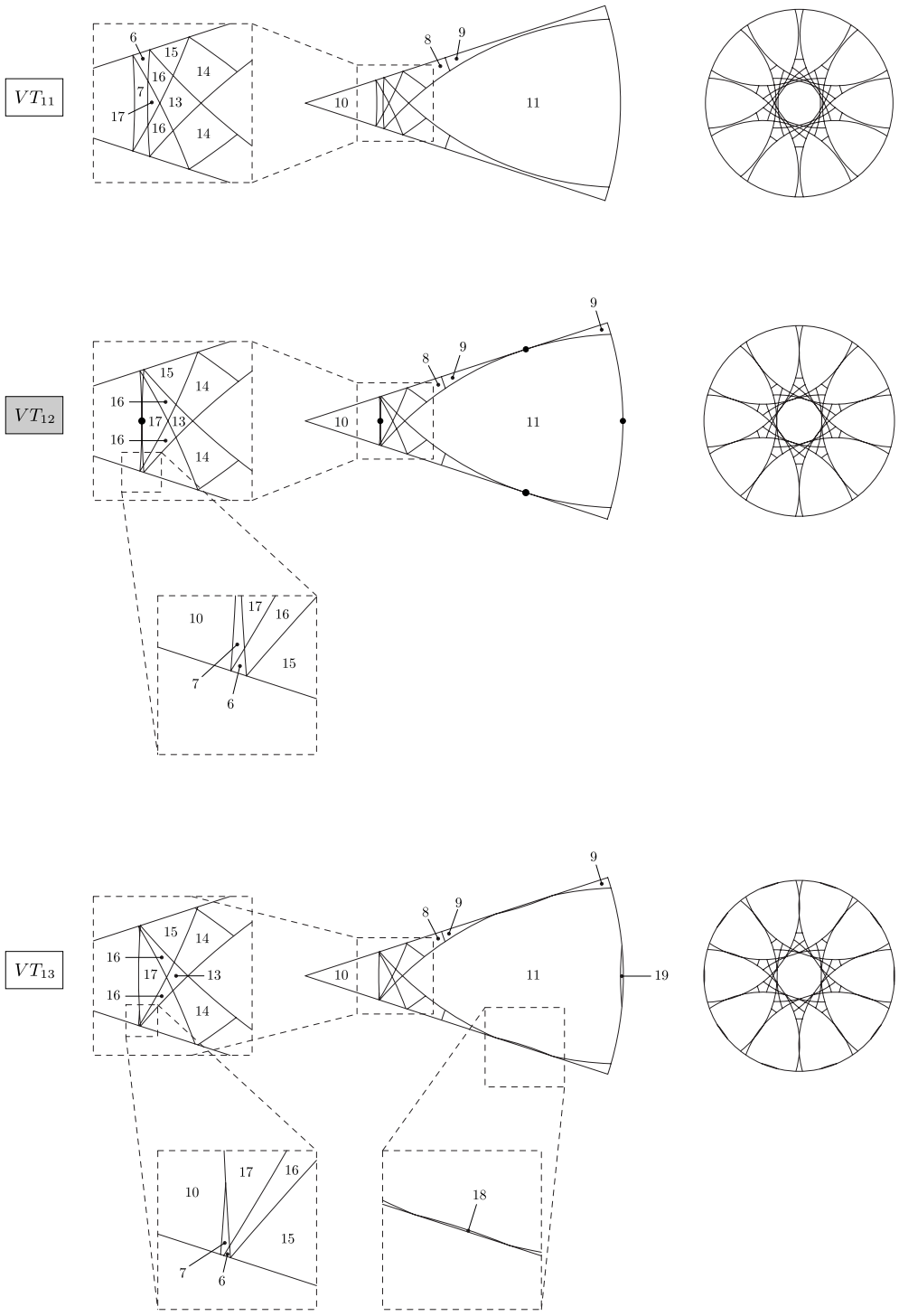

Figure 6. Division of circular acceptance windows (cases VT_{11}–VT_{13}). Each region in the acceptance window corresponds to a different Voronoi tile. The numbers which denote these regions are the numbers of Voronoi tiles from figure 12.

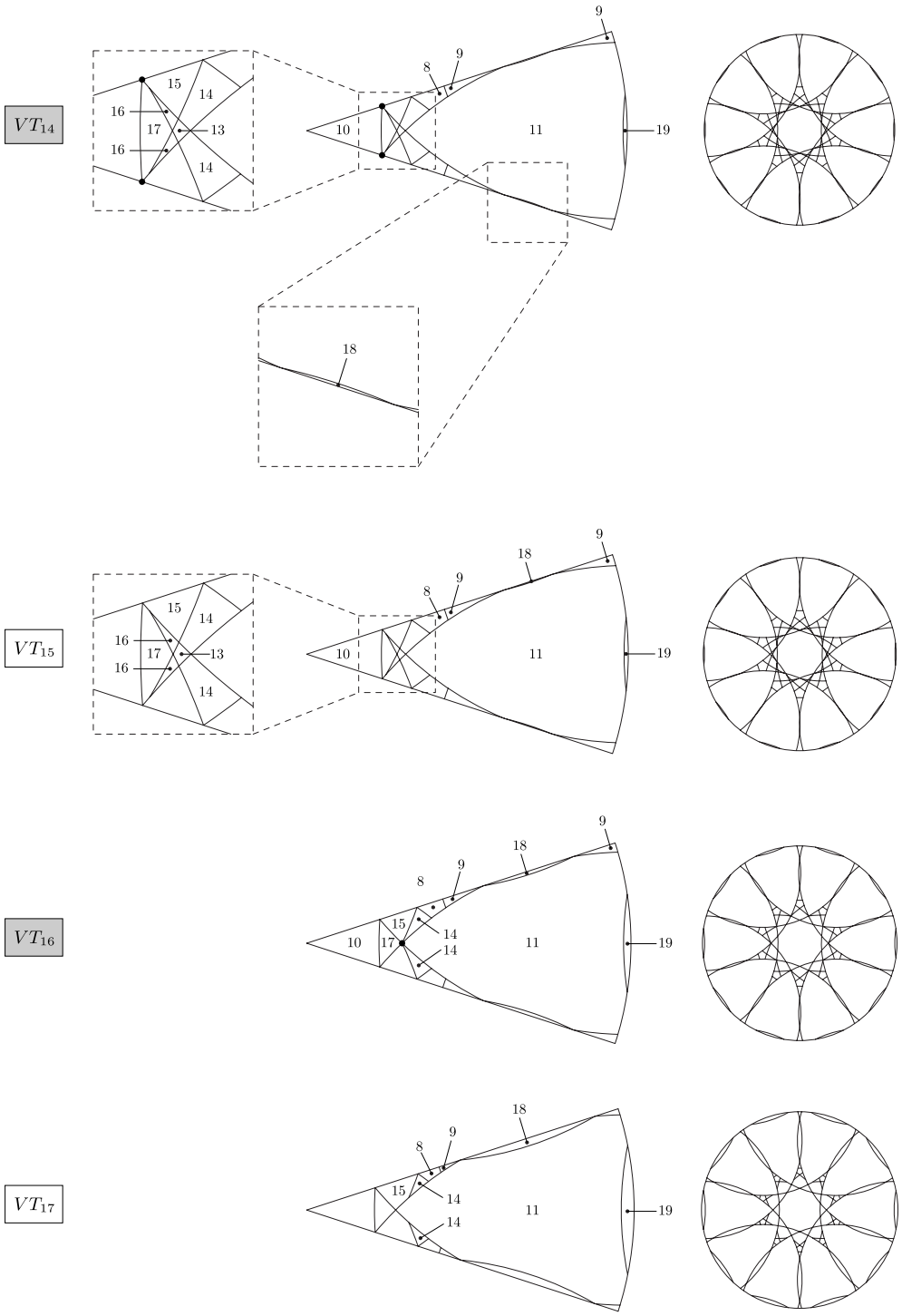

Figure 7. Division of circular acceptance windows (cases VT_{14}–VT_{17}). Each region in the acceptance window corresponds to a different Voronoi tile. The numbers which denote these regions are the numbers of Voronoi tiles from figure 12.

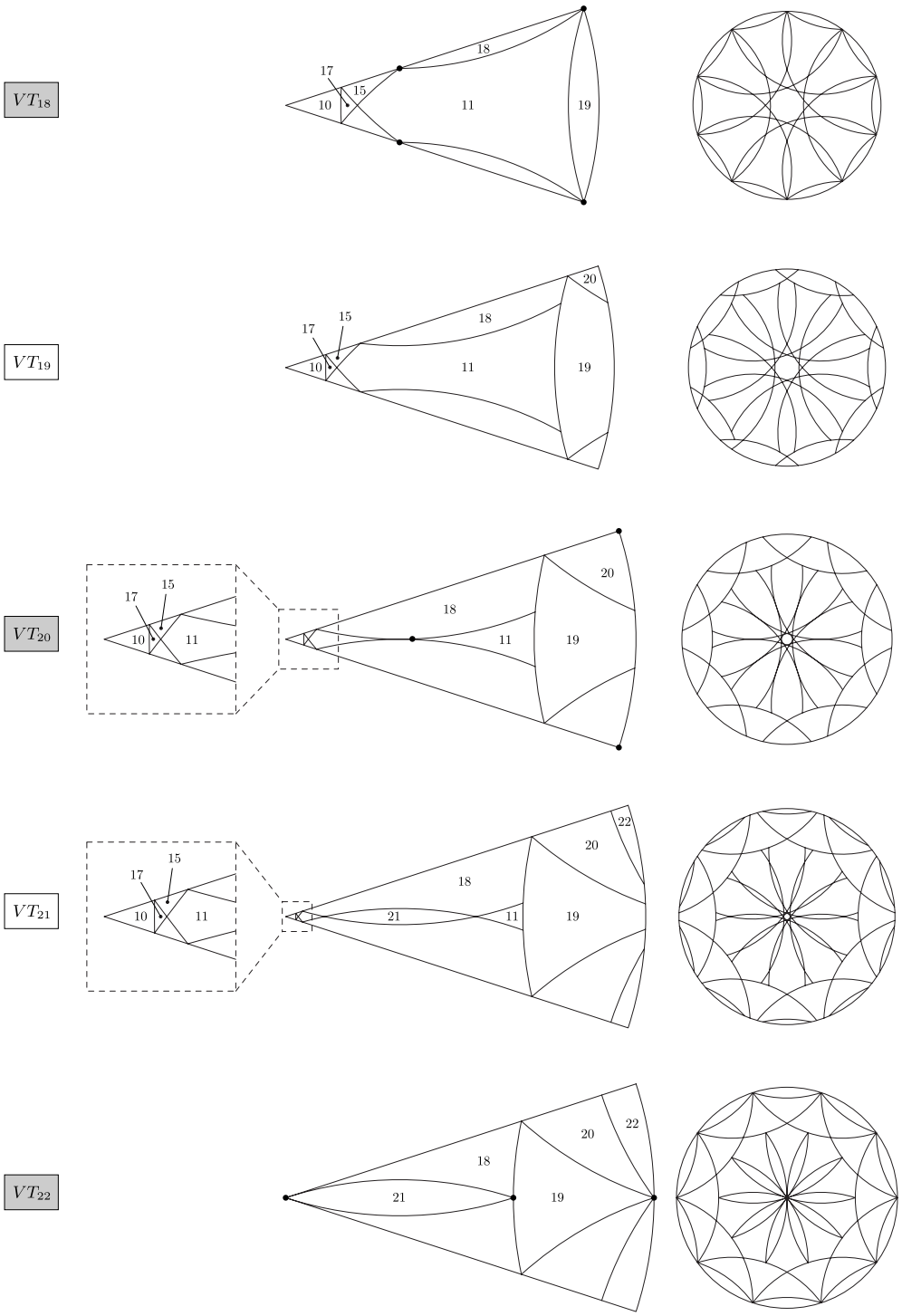

Figure 8. Division of circular acceptance windows (cases VT_{18}–VT_{22}). Each region in the acceptance window corresponds to a different Voronoi tile. The numbers which denote these regions are the numbers of Voronoi tiles from figure 12.

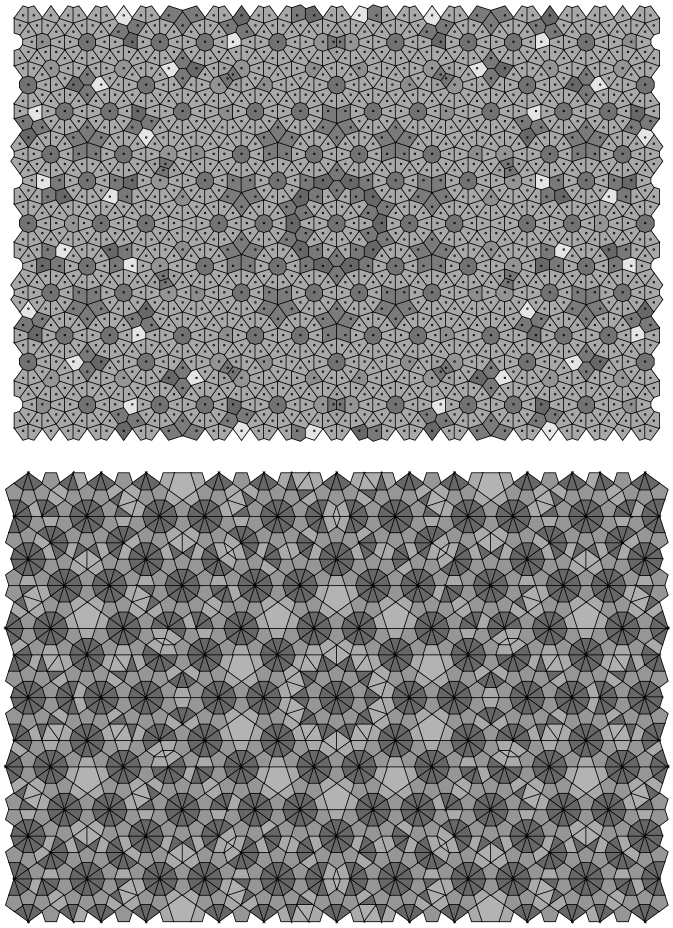

Figure 9. Voronoi and Delone tilings of a quasicrystal with the circular acceptance window for cases VT_{13} and DT_3. The radius of the acceptance window is $r = \tau/2 + 1/\tau^{13}$. This is a non-singular case which has the largest number of Voronoi tiles. But unfortunately 11 have very high density.

Delone tiles form only a subset of singular cases of VT. The complete list of the Delone singular cases DT is presented in table 2.

5. Symmetries

In this section we discuss symmetries of quasicrystals with circular acceptance window that reflect the symmetries of the Voronoi and Delone tiles. If a symmetry is observed in the division of the acceptance window, and consequently in the tiling, the lattice $M = \mathbb{Z}\Delta_2$ must also be invariant under this symmetry. Obviously a disc window centred at the origin and the lattice $\mathbb{Z}\Delta_2$ have the following symmetries:

(1) rotations around the angle $2\pi/10$,
(2) reflections along the roots from Δ_2,
(3) reflections along the lines passing thorough the origin and perpendicular to the roots from Δ_2.

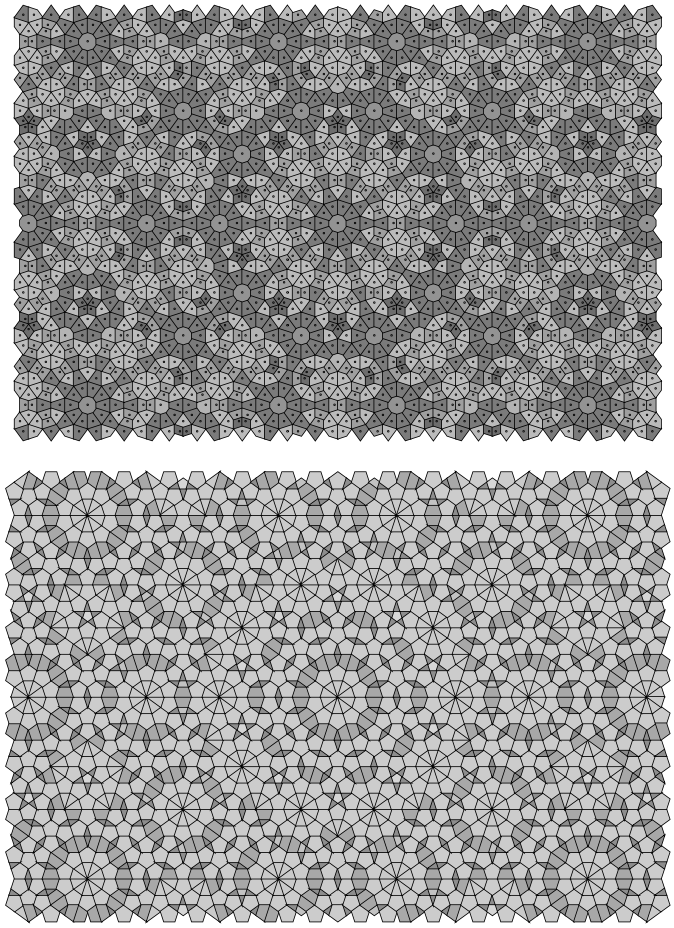

Figure 10. Voronoi and Delone tilings of a quasicrystal with the circular acceptance window for cases VT_{19} and DT_5. The radius of the acceptance window is $r = \tau/\Delta + 1/\tau^6$. This is a non-singular case.

Note that all these mappings can be generated only by two reflections: one along the horizontal line and second by the line rotated by the angle $2\pi/20$. These two reflections generate the well-known dihedral group of order 20, i.e. D_{20}. This group contains 20 elements, ten of them are reflections, the other ten are rotations.

Generally, if the acceptance window is symmetric with respect to a reflection from D_{20}, the quasicrystal is symmetric with respect to another reflection from D_{20}; the same holds for rotational symmetries from D_{20}. Therefore, each Voronoi and also Delone tile may appear in 20 orientations in the quasicrystal (10 rotations and 10 reflections). However, certain tiles are invariant under some of these transformations, reflections in particular. Hence some of the 20 orientations for these tiles coincide.

In the case of Voronoi tiling the symmetric tiles can be easily determined by observing the positions of corresponding regions in the acceptance window. Denote by R_1 a mirror of the first generator of the group D_{20}—the horizontal line—and denote by R_2 a mirror of the second generator of D_{20}—the horizontal line rotated by the angle $\pi/10$ around the origin.

If a region of a given Voronoi tile lies between these two mirrors, then obviously it has 20 copies in the acceptance window. Examples can be found in figures 4–8, e.g., tiles 12, 14

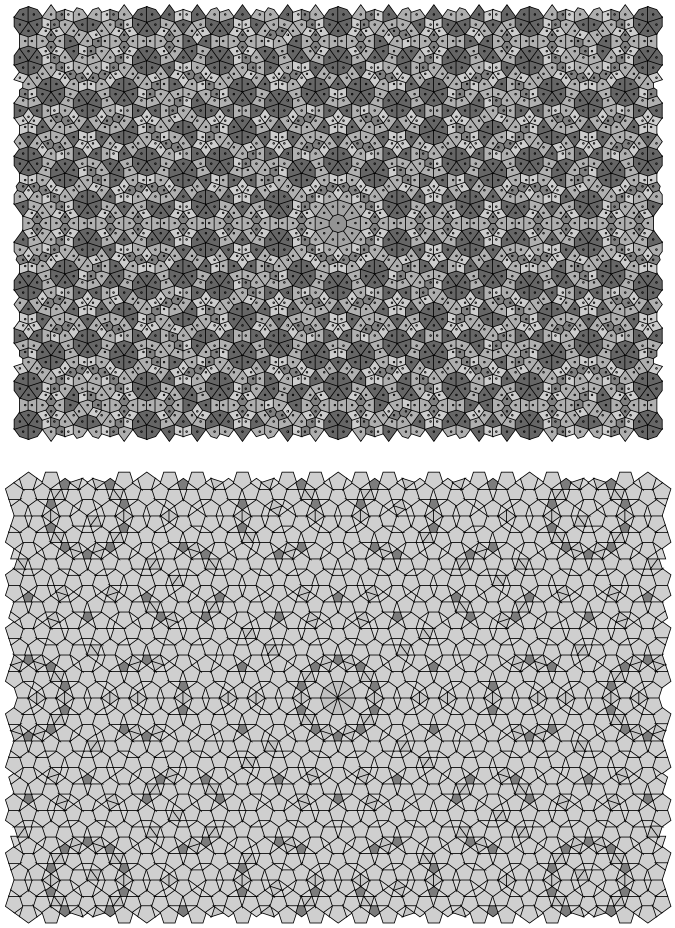

Figure 11. Voronoi and Delone tilings of a quasicrystal with a circular acceptance window for cases VT_{22} and DT_8. This is the 'mostly' singular case where $r = 1$.

and 16, which are not invariant under any of the transformations from D_{20}. Otherwise if the region lies either on R_1 or R_2 there are ten copies of the corresponding tile. An exception is the tile 10—the regular decagon—invariant under all transformations from D_{20}.

The situation for Delone tiles is slightly more complicated because we cannot derive this information from the division of the acceptance window. There are only four shapes of Delone tiles, see figure 13. Applying D_{20} to the pentagon we obtain only two different orientations. Analogously, applying D_{20} to the rest of the tiles we obtain ten orientations of each. It is not difficult to check the occurrence of these tiles in the Delone tiling of quasicrystals.

6. Summary of the results

In general, the circular acceptance window case is the most complicated among the three we consider [1, 2]. There is a larger number of Voronoi and Delone sets of tiles we have to list, and comparable sets typically contain larger number of tiles than those in the case of an equilateral decagon or rhombus.

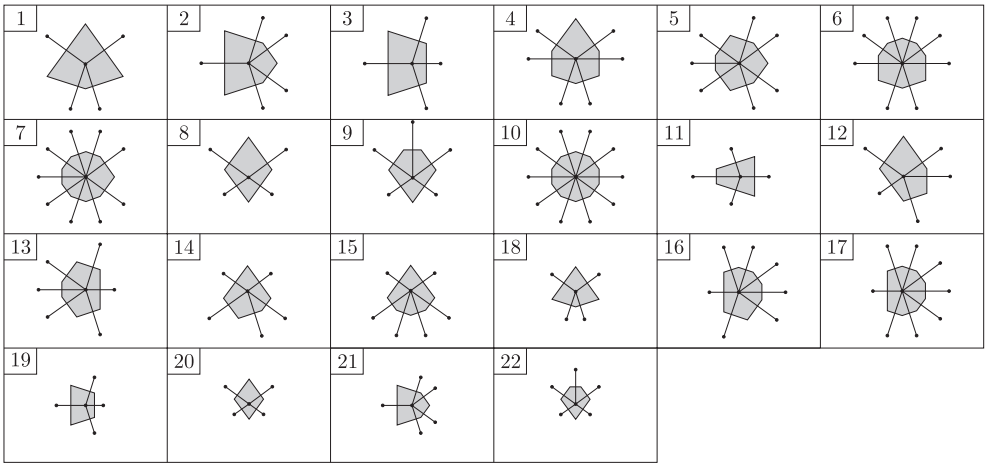

	1	2	3	4	5	6	7	8	9	10	11	12	13	14	15	16	17	18	19	20	21	22
VT_1	•	•	•	•	•	•	•	•	•	•	•											
VT_2		•	•	•	•	•	•	•	•	•	•											
VT_3		•	•	•	•	•	•	•	•	•	•	•										
VT_4			•	•	•	•	•	•	•	•	•	•										
VT_5			•	•	•	•	•	•	•	•	•	•	•									
VT_6				•	•	•	•	•	•	•	•	•	•									
VT_7				•	•	•	•	•	•	•	•	•	•	•								
VT_8					•	•	•	•	•	•	•		•	•								
VT_9					•	•	•	•	•	•	•		•	•	•	•						
VT_{10}						•	•	•	•	•	•		•	•	•	•						
VT_{11}						•	•	•	•	•	•		•	•	•	•	•					
VT_{12}						•	•	•	•	•	•		•	•	•	•	•					
VT_{13}						•	•	•	•	•	•		•	•	•	•	•	•	•			
VT_{14}								•	•	•	•		•	•	•	•	•	•	•			
VT_{15}								•	•	•	•		•	•	•	•	•	•	•			
VT_{16}								•	•	•	•			•	•		•	•	•			
VT_{17}								•	•	•	•			•	•		•	•	•			
VT_{18}										•	•				•		•	•	•			
VT_{19}										•	•				•		•	•	•	•		
VT_{20}										•	•				•		•	•	•	•		
VT_{21}										•	•				•		•	•	•	•	•	•
VT_{22}																		•	•	•	•	•

Figure 12. The 22 tiles shown at the top comprise the complete set of Voronoi tiles encountered in all quasicrystals with circular window. Shapes and relative sizes of the tiles are maintained. Also shown are the points of the quasicrystal which define the tile. For a fixed radius r of the circular acceptance window, only a subset VT_m of tiles is present in the Voronoi tiling. The entries at the intersection of a column k and a row VT_m indicate the presence of the tile number k in the set VT_m. With each tile there are at most 20 differently oriented copies in tiling according to dihedral group H_{20}. But tiles which are symmetric themselves to some subgroup appear in smaller numbers. For more details see the text.

The Voronoi and Delone tiling for quasicrystals with circular acceptance window having any radius r within the range $(\tau^{-1}, 1]$ can be identified with a Voronoi tiling set VT_j, $j = 1, \ldots, 22$, and a Delone tiling set $DT_k, k = 1, \ldots, 8$ (see figures 12 and 13). The sets VT_j and DT_k with even indices j and k are the singular sets. They occur in the tiling of

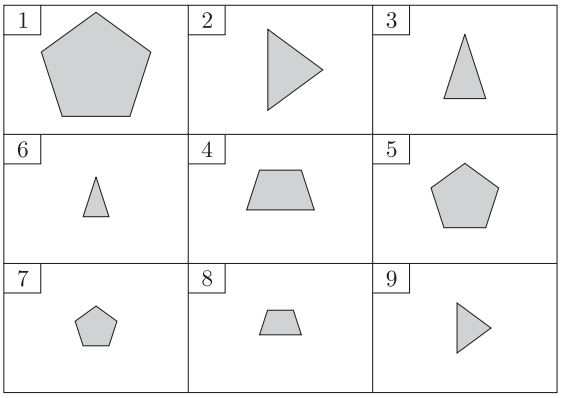

	1	2	3	4	5	6	7	8	9
DT_1	•	•	•	•	•				
DT_2	•	•	•	•	•	•			
DT_3	•	•	•	•	•	•			
DT_4			•	•	•	•			
DT_5			•	•	•	•	•	•	
DT_6			•	•	•	•	•	•	
DT_7			•	•	•	•	•	•	•
DT_8					•	•	•	•	•

Figure 13. The nine tiles shown in the top table comprise the complete set of Delone tiles encountered in all quasicrystals with circular window. Shapes and relative sizes of the tiles are maintained. For a radius r of the circular acceptance window, only a subset DT_m of tiles is present in the Voronoi tiling. The entries at the intersection of a column k and a row DT_m indicate the presence of the tile number k in the set DT_m. With each tile there are at most 20 differently oriented copies in tiling according to dihedral group H_{20}. But tiles which are symmetric themselves to some subgroup appear in smaller numbers. For more details see the text.

quasicrystals with a precise value of the radius of its acceptance window (disc). The values are listed in table 2, and their relative position is shown graphically in figure 3 by the black dots in the interval $(\tau^{-1}, 1]$. The radii between two adjacent dots refer to the acceptance windows of quasicrystals with the (odd-numbered) non-singular tiling sets VT_j and DT_k.

A quasicrystal has singular tiling sets VT_j and DT_k, if an arbitrary small change in the size of its acceptance window (radius of the disc) leads to distinct tiling sets VT_{j+1}, VT_{j-1} and DT_{k+1}, DT_{k-1}. Otherwise, the tiling set is non-singular.

The neighbours of a quasicrystal point $x \in \Sigma(\Omega)$ are those points in $\Sigma(\Omega)$ which influence the shape of the Voronoi tile of x. A numbered list of distinct Voronoi tiles together with the neighbours of the central point is shown in scale in the upper part of figure 12. Twenty orientations of the tiles are possible, due to the D_{20} symmetry of the quasicrystal $\Sigma(\Omega)$. A tiling set VT_j consists of the tiles marked by a black dot in the lower part of figure 12. Analogous results concerning the set of Delone tiles, and the subsets DT_k are found in figure 13.

Figures 4–8 show the divisions of the circular acceptance window into regions containing those points $x^* \in \Omega$ for which the Voronoi cell $V(x)$ has the same shape and orientation. Each case VT_j is illustrated with the disc of the acceptance window and a segment of the disc. The numbers of regions coincide with the numbers of corresponding tiles in figure 12. The

figures illustrating the sets VT_j with odd index j represent a typical division of the acceptance window. Continuous change of the radius of the disc would continuously change the regions but the set of tiles remains the same, until a singular value of the radius is reached. In that case the tiling set becomes VT_{j-1} (for decreasing r) or VT_{j+1} (for increasing r).

All the tiles in our list have the density of occurrence within their tiling >0. Equivalently, the area corresponding to such tiles in the acceptance window is >0. Under certain circumstances special tiles whose density is 0 may appear in a tiling. As was explained in section 4, it depends on the intersection of the boundary of the acceptance window with the $\mathbb{Z}[\tau]$-lattice M and the fact whether Ω is a closed or open region. The situation for the case of a circular acceptance window is not complicated, since the intersection of the boundary with M is at most a finite set. When this is not the case (for example, decagonal acceptance window [2]), a detailed analysis of occurrences of tiles with zero density depending on the boundary would be needed.

Acknowledgments

We are grateful to E Pelantová for useful suggestions. ZM and JZ are grateful for the hospitality of the Centre de recherches mathématiques, Université de Montréal, where a part of the work was done. We acknowledge the financial support of the Grant Agency of the Czech Republic GA ČR 201/01/0130, NSERC Canada and FCAR of Québec.

References

[1] Masáková Z, Patera J and Zich J 2002 Classification of Voronoi and Delone tiles in quasicrystals: I. General method **36** 1869–94

[2] Masáková Z, Patera J and Zich J 2003 Classification of Voronoi and Delone tiles in quasicrystals: III. Decagonal acceptance window of arbitrary size *Preprint* CRM

[3] Moody R V and Patera J 1993 Quasicrystals and icosians *J. Phys. A: Math. Gen.* **26** 2829–53

[4] Pelantová E and Perelomov A M 1998 Diophantine equations related to quasicrystals: a note *Theor. Math. Phys.* **115** 737–9

[5] Zich J 1993 Tilings *Handbook of Convex Geometry* ed P M Gruber and J M Willis (Amsterdam: Elsevier)